Assessing the reactivity of Fe(II) sorbed on smectite clays: U(VI) reduction

Chakraborty, S.; Banerjee, D.; Scheinost, A.; Grenèche, J.-M.; Favre, F.; Géhin, A.; Charlet, L.;

Originally published:

April 2023

Journal of Materials Research 38(2023), 2752-2763

DOI: https://doi.org/10.1557/s43578-023-00998-8

Assessing the reactivity of Fe(II) sorbed on smectite clays: U(VI) reduction

Journal:	*Environmental Science & Technology*
Manuscript ID	es-2019-068495
Manuscript Type:	Article
Date Submitted by the Author:	12-Nov-2019
Complete List of Authors:	Chakraborty, Sudipta; Kanchrapara College, Department of Chemistry Banerjee, Dipanjan; KU Leuven, Department of Chemistry Scheinost, Andreas; The Rossendorf Beamline (BM20), European Synchrotron Radiation Lab Grenèche, Jean-Marc; Université du Maine, Institut des Molécules et Matériaux du Mans Favre, Fabienne; Ecole d'ingenieurs et architectes de Fribourg, Civil Engeniering Géhin, Antoine; University Grenoble Alpes, ISTerre, Environmental Geochemistry Group, Observatory for Earth and Planetary Sciences Charlet, Laurent; Institut des Sciences de la Terre,

Assessing the reactivity of Fe(II) sorbed on smectite clays: U(VI) reduction

Sudipta Chakraborty,[*,1,5] Dipanjan Banerjee,[2] Andreas C. Scheinost,[3]
Jean-Marc Grenèche,[4] Fabienne Favre,[1,6] Antoine Géhin,[1] Laurent Charlet [1]

[1] ISTerre, Environmental Geochemistry Group, Observatory for Earth and Planetary Sciences, Grenoble University, 38041 Grenoble Cedex 9, France

[2] Dutch-Belgian Beamline (DUBBLE), European Synchrotron Radiation Facility, 71 avenue des Martyrs, CS 40220, 38043 Grenoble Cedex 9, France

[3] Institute of Resource Ecology, Helmholtz-Zentrum Dresden - Rossendorf, Dresden, Germany

[4] Institut des Molécules et Matériaux du Mans, IMMM, UMR CNRS 6283, Université du Maine, 72085 Le Mans Cedex, France

[5] Department of Chemistry, Kanchrapara College, West Bengal, India

[6] ITEC, HEIA-FR, HES-SO, University of Applied Sciences Western Switzerland, CH-1700, Fribourg

chakrabortysudipta@hotmail.com; banerjee@esrf.fr; scheinost@esrf.fr; jean-marc.greneche@univ-lemans.fr; Fabienne.Favre@hefr.ch; antoine.gehin@wanadoo.fr; charlet38@gmail.com

* CORRESPONDING AUTHOR

Phone: +91 33 2585 8790; fax: +91 33 2826 3164; e-mail: chakrabortysudipta@hotmail.com

ABSTRACT

The reactivity of Fe(II) sorbed on three Ca-exchanged smectite clays was probed via U(VI) reduction at pH 6.0 (± 0.2) under CO_2-free, anoxic (O_2 <1 ppmv) condition. The clays varied with regard to structural Fe content from Fe-free (0 wt.%) montmorillonite (MONT), to Fe-poor (2.6 wt.%) montmorillonite (Fe-MONT), to Fe-rich (25.8 wt.%) nontronite (NAu-2). The U L_{III}-edge XANES spectra showed no reduction of U(VI) in presence of Fe(II) sorbed on either Fe-MONT or NAu-2 after 72 h but a partial reduction (21%) on MONT after 24 h. U L_{III}-edge EXAFS spectra further showed the formation of a soddyite-like surface precipitate on MONT in presence of sorbed Fe(II) after 72 h. The Mössbauer data further reveals that 10 (± 2) % of the total sorbed Fe(II) was oxidized in presence of MONT before and an additional 6 (± 2) % after addition of U(VI). The mechanism of U(VI) reduction involves Fe(II) specifically sorbed on oxidized and reduced strong edge sites of MONT. The non-reactivity of Fe(II) sorbed on Fe-MONT and NAu-2 towards U(VI) reduction is likely linked to the inter-valence charge transfer (IVCT) between surface Fe(II) and structural Fe(III). The present study demonstrates that the reduction capacity of Fe bound to the surface depends strongly on the nature of clay and correspondingly on the oxidation state of the sorbed Fe. Thus Fe(II) sorbed clay cannot be always considered as "universal reductant" for U(VI).

BRIEF: Clay catalyzed redox processes between aqueous U(VI) and surface bound Fe(II).

Introduction

The mobility and transport of hexavalent uranium, U(VI) in presence of clay have been studied for many years as possible remediation options in areas contaminated by uranium as well as for the evaluation of the performance of highly radioactive nuclear wastes (HLNW) repositories. As Fe(II) is common in both environments, the possible reduction of U(VI) to U(IV) and a comprehensive understanding of the Fe(II)-U(VI)-clay ternary system is necessary to mitigate the future possible risk in an anoxic uranium-polluted subsurface and to ensure long term stability of uranium at underground waste disposal sites.

Montmorillonite and nontronite are members of the smectite sub-group clay with structures similar to 2:1 phyllosilicates and are known to sorb Fe(II) and U(VI) present in solution. The mechanisms of U(VI) sorption on montmorillonite have been extensively investigated using surface complexation modeling,[1-6] spectroscopic analysis and molecular dynamics simulation methods,[7-14] while the information available on the nontronite system is limited.[15-17] Surface-bound Fe(II) commonly behaves as stronger reductant than corresponding aqueous species in both biotic and abiotic pathways, and therefore can transform organic (nitroaromatic explosives, pesticides and polyhalogenated solvents) and inorganic (Cr, Tc, Se, U) pollutants into nontoxic forms.[18-20]

The sorption of Fe(II) on montmorillonite has been well documented.[21-23] The sorption affinity of pH-dependent montmorillonite makes it possible to distinguish three types of edge sites: weak sites, oxidized strong sites and reduced strong sites. Strong “oxidized” sites refer to those that are linked with heterogeneous surface oxidation of Fe(II), while on strong “reduced” and weak sites only sorption takes place.[21,23] The sorption of Fe(II) on iron-rich nontronite (NAu-1 & NAu-2) has been studied in detail by Tsarev et al.[15] and Jaisi et al.[24]. In addition to pH dependence, both montmorillonite and nontronite undergo heterogeneous surface oxidation of sorbed Fe(II) via different mechanisms. In montmorillonite, surface oxidation of Fe(II) may result in the formation of ferric hydroxide and lepidocrocite at lower and higher pH respectively[25] which, however, coupled to catalyze the reduction of U(VI),[15,25] Se(IV),[19] 4-chloronitrobenzene.[26,27] In the case of surface oxidation of Fe(II) on structural Fe(III)-bearing smectites, Fe(III)-montmorillonite and nontronite have a unique characteristic known as inter-valence charge transfer (ICVT) between sorbed Fe(II) and structural Fe(III). It has been proposed that Fe(III), which exists in clay tetrahedral (nontronite) and/or octahedral (montmorillonite) sites participates in the electron transfer reaction by a charge-shuttling process for redox mediation and catalysis or by edge and basal sites. Therefore, various secondary mineral phases like green rust, ferrihydrite, lepidocrocite and magnetite may be formed as oxidation products.[28-31] The reactivity of sorbed Fe(II) on structural Fe(III) bearing clays has been shown to vary in different cases. Jones et al.[27] observed a significant decrease of reactivity of Fe(II) sorbed on nontronite after 18 days in reduction of 4-chloronitrobenzene. Tsarev et al.[15] observed a partial reduction of U(VI) by Fe(II) sorbed on nontronite (NAu-1 and NAu-2) in presence of CO_2 while a partial oxidation of As(III) to As(V) was reported by Ilgen et al.[32]

Our previous study[25] has addressed the pH dependent abiotic reduction of U(VI) by Ca-exchanged montmorillonite (Fe-free, MONT) in the presence of Fe(II) and reported the formation of monomeric U(IV) as the most plausible sorbed reaction product rather than the commonly observed uraninite (UO_2). By combining U and Fe speciation (following XANES and Mössbauer analyses) in this study, we suggest an U(VI) reduction mechanism by considering specific site sorption of Fe(II) on MONT. The Fe(II) reactivity related to the surface of Fe-poor montmorillonite (2.6 wt.% Fe-MONT) and nontronite (25.6% NAu-2) was compared to that of

Fe-free montmorillonite (0 wt.% MONT) probing U(VI) as a redox sensitive species under similar experimental conditions. All the experiments were performed in a CO_2-free atmosphere to compare our results with those obtained in presence of CO_2 by Tsarev et al.[15] and also to exclude the effect of carbonate on uranium mobilization. The anoxic (O_2-free) condition should preserve the oxidation state of ferrous iron and prevent the re-oxidation of reduced uranium species. A high ionic strength (0.05M $CaCl_2$) was used to exclude Fe(II) sorption at cation exchange sites, and thus to take into account only for the reactivity of Fe(II) sorbed specifically in the reduction process.

Materials and Methods

Chemicals

All the solutions were prepared with boiled, argon (99.9992%) purged Millipore Milli-Q water. NaOH and HCl stock solutions were made from Titrisol ampoules. The Fe(II) stock solutions were freshly prepared from analytical grade $FeCl_2$, $4H_2O$ (Fluka Chemica), after transferring the required amount to a glove box (JACOMEX) under N_2 atmosphere (CO_2, O_2 <1 ppmv), dissolved in deoxygenated water (dissolved O_2 <1 mgL^{-1}) and acidified with 0.1 M HCl to pH <2 to avoid oxidation.[33] $^{57}Fe(II)$ stock solutions were prepared by dissolving ~100 mg $^{57}Fe(0)$ in concentrated HCl at 100 °C and subsequent dilution with deoxygenated water in glove box. U(VI) solutions were prepared from 1000 mgL^{-1} $UO_2(NO_3)_2.6H_2O$ (Alfa Aesar) standard solution.

Clay minerals

The synthetic Fe-free montmorillonite (MONT) ($Na_{0.30}[(Al_{1.70}Mg_{0.30})Si_4O_{10}(OH,F)_2],nH_2O$) was identical to that used in previous studies.[19,21,25] The synthetic structural Fe(III) bearing montmorillonite (Fe-MONT, 2.6 wt.% Fe) has the representative chemical formula, $Na_{0.66}(Si_{8.0})(Al_{3.00}Mg_{0.66}\,Fe_{0.34}^{III})$. The natural iron-rich nontronite (NAu-2, 25.8 wt.% Fe) $[Na_{0.72}(Si_{7.55}Al_{0.50}Fe_{0.29}^{III})(Mg_{0.05}Fe_{3.54}^{III})]$ was obtained from the Source Clay Minerals Repository, South Australia.[34] Approximately 1% calcite impurities in this clay was removed by using Na-acetate/acetic acid solution (pH 5) verified by XRD (not shown). All three clays in their Ca-exchanged forms were obtained by repeated saturation with 0.05 M aqueous solution of $CaCl_2$ and clay suspensions were then extensively argon-purged and transferred to the glove box.

Preparation of Fe(II) sorbed smectites

To evaluate the reactivity of sorbed Fe(II) on smectites, three clay suspensions (10.6 ± 0.2 gL^{-1}) were reacted with 1.2 ± 0.2 mM Fe(II) at pH 6.0 ± 0.2 for 72 h before U(VI) addition. The Mössbauer samples were prepared in a similar way using $^{57}Fe(II)$. The experimental conditions are given in Table 1.

Kinetic redox experiments

Fe(II)–U(VI) redox kinetic experiments in the presence of three Ca-exchanged smectite clays (MONT, Fe-MONT and NAu-2) were carried out in a closed reactor at room temperature (24 ± 1 °C) with 0.05 M $CaCl_2$ ionic background as described in our previous study for MONT.[25] The control samples (without Fe) containing clay and U(VI) was prepared in 50 ml vials by batch method (Table 1).

^{57}Fe Mössbauer spectrometry

^{57}Fe Mössbauer experiments were performed at 77K in transmission geometry with a 925 MBq γ-source of ^{57}Co/Rh mounted on a conventional constant acceleration drive. The samples containing about 5 mg Fe.cm^{-2} were prepared and sealed in a glove box, and then transferred in a bath cryostay. The hyperfine structures were fitted using the MOSFIT program[35] involving quadrupolar components with lorentzian lines; the isomer shift values are referred to that of α-Fe at RT. The velocity of the source was calibrated using α-Fe as the standard at RT.

X-ray absorption spectroscopy

X-ray Absorption Near-Edge Structure (XANES) and Extended X-ray Absorption Fine-Structure (EXAFS) spectra were collected at the Rossendorf Beamline at the European Synchrotron Radiation Facility (ESRF, Grenoble, France). The energy of the X-ray beam was tuned by a doubled crystal monochromator operating in pseudo channel-cut mode using a Si(111) crystal pair. Two platinum-coated Si mirrors before and after the monochromator were used to collimate the beam into the monochromator and to reject higher harmonics. Uranium L_{III}-edge spectra were collected in fluorescence mode using a 13-element high purity germanium detector (Canberra) together with a digital signal processing unit (XIA Xmap). Spectra were collected at 15K using a closed cycle He cryostat with a large fluorescence exit window (CryoVac). The energy was calibrated using the maximum of the first derivative of the yttrium K-edge (17038 eV). Between eight and ten scans were recorded for each sample. Dead time correction of the fluorescence signal, energy calibration and averaging of the individual scans were performed with the software package SixPack.[36] Normalization, transformation from energy into k space, subtraction of a spline background was performed with WinXAS using routine procedures.[37] Statistical analyses of XANES and EXAFS spectra was performed by Iterative Target-test Factor Analysis (ITFA) using the ITFA software package.[38-40]

Results and Discussion

Sorption of Fe(II) and U(VI) on clays

The experimental conditions with results from wet chemical analyses are shown in Table 1. Among three clays, NAu-2 has the highest affinity for Fe(II) sorption followed by Fe-MONT and MONT (Figure 1). The sorption of Fe(II) at pH 6 is attributed to cation exchange as well as site-specific sorption to clay edge sites.[21,26] In the absence of Fe(II), the extent of U(VI) sorption is less on Fe-MONT than MONT or Nau-2. The kinetic experiments (Fig. 1A & 1B) show a fast uptake of >80% of U(VI) from solution by the three clays with sorbed Fe(II) within 1 hr. The EXAFS results identified surface precipitation of soddyite-like phase only on MONT with sorbed Fe(II) after 72 h, a precipitate which was not observed for Fe-MONT and NAu-2. The removal of aqueous U(VI) by Fe(II) sorbed on MONT is therefore attributed primarily to a fast sorption of U(VI), followed by a slow precipitation of soddyite-like phases probably favored by dissolution of clay which will be discussed in the next section. In Fe(II) sorption experiment on NAu-2, a visible color change is observed from brown to pale green clearly different from commonly observed the deep green color of dithionite reduced NAu-2 (Figure S1 in supporting information). This color change is attributed to inter-valence charge transfer (IVCT) between sorbed Fe(II) and structural Fe(III) reported by other investigations.[15, 28, 29]

Speciation of uranium in presence of Fe(II) sorbed on clays

XANES and EXAFS

The normalized XANES spectrum of the U(VI) reference sample (NAu-2 + U(VI) at pH 6.2 i.e. N1) (Table 1) in Figure 2A shows the characteristic features of the uranyl ($U^{VI}O_2^{2+}$) structure, including a white line peak centered at 17179 eV and a shoulder centered at approximately 17190 eV. The feature at 17190 eV has previously been shown to result from multiple scattering resonances of the linear uranyl ion structure with the short U-O_{ax} bonds.[42] The XANES spectra of M1, M2, M3, F1, F2 and N2 samples are very similar to the U(VI) reference, implying that the dominating phase of uranium in these samples is in +VI oxidation state. This visual observation of the XANES spectra was further statistically verified with ITFA and a U(IV) reference spectrum, showing no coincidence. Therefore, no reduction of U(VI) by Fe(II) sorbed on three clays was observed after 72 h. ITFA analysis of the k^3-weighted EXAFS spectra revealed the presence of two structurally different components or species. One of the components, prevailing in samples M2 and M3, could be identified as samples an amorphous, soddyite [$(UO_2)_2SiO_4.2H_2O$]-like surface precipitate forming in presence of Fe(II) on MONT. Using the spectrum of M1 as representative of the most likely pure U(VI) sorption complex, and that of a soddyite reference as representative of the surface precipitate, we could derive by Iterative Target Test the quantitative speciation of both components in the other sample spectra (Table 2). Only the M series starting after 24 h and increasing with reaction time showed evidence of surface precipitation. For samples F2 and N2, no reduction of U(VI) to lower valence state occurred suggesting that sorbed Fe(II) probably loses its reactivity while being involved in intervalence charge transfer (IVCT) with structural Fe(III) present in tetrahedral and/or octahedral sites for Fe-MONT and NAu-2 clays before reacting with aqueous U(VI).

To focus more on the kinetics of surface precipitation, we analyzed three samples M2a, M2b and M2c reacted at different time intervals. The XANES and EXAFS quantification (Table 2, 3) shows that neither reduction of U(VI) nor surface precipitation occurred (Table 1) before 24 h in case of M2a and M2b. However, a partial reduction about 21% of total sorbed U(VI) was indicated by XANES in M2c (Table 3). However, the spectral characteristic of M2c with its absence of U-U backscattering is not similar to that of U_3O_8(s) with mixed U valence used as reference (not shown). Although we cannot unequivocally prove the presence of U-Al or U-Fe backscattering paths most likely masked by the strong multiple scattering peak at 2.9 Å (uncorrected for phase shift), the spectral features of M2c are in line with the formation of an inner-sphere complex like ≡Fe(II)-O-U(VI) at the "reduced strong" edge sites coupled to a slow reduction step attributed to the surface oxidation of Fe(II) at the "oxidised strong" edge sites of MONT. No further increase in U(VI) reduction is observed before 72 hr. Moreover, in samples M2 and M3 we did not observe any U(VI) reduction probably due to the fact that surface precipitation starts between 24 h and 72 h and is clearly visible after 72 h (Figure 2 & 3). The total Si concentrations in solution in samples M2a, M2b and M2c show a slight upward trend up to 24 h due to the dissolution of MONT which, however, decreases in sample M2 due to surface precipitation of an uranium silicate-like soddyite solid phases (Table 3). So it is possible that the major part of the signals comes from the U(VI) bearing soddyite-like mineral phase showing no reduction in M2 and M3.

Speciation of sorbed Fe on clays with/out U(VI)

Mössbauer analyses

The 77K Mössbauer spectra of Fe(II) sorbed on MONT before and Figure 4B after U(VI) addition are compared in Figure 4. The corresponding refined values of the hyperfine parameters are listed in Table 4. According to the values of isomer shift, among four doublets, D1, D2 and

D3 are unambiguously assigned to Fe(II) species while D4 to Fe(III) species. The spectrum in Figure 4A must be deconvoluted into four quadrupolar doublets corresponding to (a) exchangeable $FeCl^+$, (b) exchangeable Fe(II), (c) Fe(II) sorbed on strong reduced site2 and (d) Fe(II) sorbed on strong oxidized site of MONT.[21] The presence of Fe(III) (D4 doublet) in sample M suggests that 10% of total sorbed Fe(II) is oxidized to Fe(III) by "oxidized strong edge sites" of MONT surface before U(VI) addition. This finding is well consistent with that previously found by Charlet et al.[19] and Gehin et al.[21] The spectrum shown in Figure 4B must be deconvoluted into at least five doublets. The new doublet D5 with higher quadrupole splitting value is assigned to the Fe(III) sorbed on strong reduced site2 which appeared to the detriment of the oxidation of sorbed Fe(II) of the "strong reduced" site2 of MONT after addition of U(VI). Thus the additional 6% oxidation of Fe(II) involves "strong reduced edge sites" concerned by the U(VI) reduction. On the basis of this result, two mechanisms of U(VI) reduction are proposed.

Mechanistic approaches of U(VI) sorption-reduction by Fe(II)/MONT

Our previous study[25] has shown that reduced uranium may exist on MONT and results in surface monomeric U(IV) complex species also shown in recent studies.[15] Therefore, U(VI) reduction mechanism is suggested by considering U(VI) and monomeric U(IV) surface complexes formed with Fe(II) specifically sorbed on oxidized and reduced strong sites of MONT. Furthermore, Mössbauer analyses of solid phase Fe speciation (Table 4) reveals that the reduction of U(VI) occurs in two steps: (1) a slow, diffusion controlled process involving H_2-like species formation resulting from the pre-oxidation of Fe(II) on oxidized strong sites of MONT[19] and (2) a relatively faster electron transfer to U(VI) through inner-sphere complexation between U(VI) and Fe(II) sorbed on "reduced" strong sites of MONT.

Mechanism 1. U(VI) reduction into monomeric U(IV) sorbed species by surface H_2 species produced due to pre-oxidation of Fe(II) specifically sorbed on MONT oxidized strong sites.[19,21,42]

$$Fe^{2+}(aq) + s^1\equiv^{3+}(OH^-)_3 \longrightarrow s^1\equiv^{3+}(OH^-)(O^{2-})_2Fe^{2+} + 2H^+ \quad (1)$$

$$s^1\equiv^{3+}(OH^-)(O^{2-})_2Fe^{2+} + 2H_2O \leftrightarrow s^1\equiv^{3+}(O^{2-})_3Fe^{3+}(OH^-)_2 \ldots.(H_2)_{0.5} + 2H^+ \quad (2)$$

$$s^1\equiv^{3+}(O^{2-})_3Fe^{3+}(OH^-)_2 + 2s^1\equiv^{3+}(O^{2-})_3Fe^{3+}(OH^-)_2 \ldots.(H_2)_{0.5} + 2U^{VI}O_2^{2+} + 2H_2O \longrightarrow$$

$$(s^1\equiv^{3+}(O^{2-})_3Fe^{3+}(OH^-)_2)U^{VI}O_2(OH)_2 + (s^1\equiv^{3+}(O^{2-})_3Fe^{3+}(OH^-)_2)_2U^{IV}(OH)_2 + 2H^+ \quad (3)$$

Mechanism 2. U(VI) reduction by Fe(II) sorbed on reduced strong sites of MONT by inner-sphere complex formation.

$$Fe^{2+}(aq) + s^2\equiv^{3+}(OH^-)_3 \rightarrow s^2\equiv^{3+}(OH^-)(O^{2-})_2Fe^{2+} + 2H^+ \quad (4)$$

$$2s^2\equiv^{3+}(OH^-)(O^{2-})_2Fe^{2+} + U^{VI}O_2^{2+} + 4H_2O \rightarrow (s^2\equiv^{3+}(O^{2-})_3Fe^{3+}(OH^-)_2)_2U^{IV}(OH)_2 + 4H^+ \quad (5)$$

where $s^1\equiv^{3+}(OH^-)_3$ and $s^2\equiv^{3+}(OH^-)_3$ represent one mole of MONT oxidized and reduced strong sites respectively at pH 6. Equation (3) is attributed to a diffusion controlled process and is therefore slow (days).

Precipitation of Soddyite-like mineral phase on Fe(II) sorbed on MONT surface

M2 and M3 suspensions are slightly oversaturated with respect to soddyite (saturation index 0.37) and precipitation may occur (Table 2) according to:

$$2U^{VI}O_2^{2+} + H_4SiO_4 + 2H_2O = (U^{VI}O_2)_2SiO_4.2H_2O + 4H^+ \quad (6)$$

Previously it has been shown that redox potential of mineral/electrolyte suspension is useful in predicting end product reactivity of mineral when reacted with a contaminant.[15,43] In the present study, the redox potential of Fe(II) sorbed on Fe-MONT or NAu-2 suspension is lower than Fe(II)/Fe(III) in solution (Figure S2 in supporting information). Moreover, the amount of Fe(II) sorbed on these clays is nearly 10 times higher than the amount of sorbed U(VI), 5 times higher than stoichiometry would require for complete reduction to occur. However U(VI) reduction is not complete. In MONT 16% of the total sorbed Fe(II) is found to be active in electron transfer to U(VI). On the other hand, Fe(II) sorbed on Fe-MONT and NAu-2 shows stronger affinity to reduce structural Fe(III) before U(VI) addition and therefore loses its reactivity towards U(VI) reduction. One may form "dead-end" –Fe(III)-O-U(VI) complexes at both of these clay surfaces.

Working at higher concentration of clay, Fe(II) and U(VI) than those we previously used,[25] we do not show significant impact on the extent of U(VI) reduction but we observe a precipitation of soddyite-like phases on MONT. However, such precipitation is not observed in other systems containing either U(VI)-Fe(III)-bearing clays or Fe(II)-U(VI)-Fe(III)-bearing clays. It can therefore be concluded that the mobility of U(VI) is controlled by a coupled sorption-reduction and uranium silicate mineral phase precipitation reaction in the U(VI)-Fe(II)-MONT system whereas only redox-inactive sorption prevails when U(VI) is co-adsorbed on Fe(II)-Fe-MONT and Fe(II)-NAu-2 systems.

Environmental implications

The long-term stability of uranium present in nuclear waste disposal sites or bomb shells must be carefully assessed using MONT, Fe-MONT and NAu-2 considering that (1) mobility of U(VI) is mainly controlled by sorption-reduction on Fe(II) sorbed MONT surface coupled with the precipitation of soddyite-like solids at higher U concentrations and (2) the reductive immobilization of U(VI) is not operative in Fe(II)-U(VI)-Fe-MONT and Fe(II)-U(VI)-NAu-2 systems due to inter-valence charge transfer.

ACKNOWLEDGMENT

This research was funded by ANDRA (project no. #20072484). We are thankful to Dr. Jocelyne Brendlé for synthesis of Fe-MONT and Dr. Laura Leone for Mössbauer analysis of Fe-MONT. Delphine Tisserand and Florian Molton are acknowledged for their technical support within the Analytical Chemistry Platform at ISTerre (OSUG), the ESRF Radioprotection Group and the scientists of the Rossendorf Beamline (ROBL) for providing support during the XAS measurements.

Literature Cited

(1) Bachmaf, S; Merkel, B. Sorption of U(VI) at the clay mineral-water interface. *Environ. Earth Sci.* **2010**, 63 (5), 925-934.

(2) Bradbury, M.; Baeyens, B. Modelling the sorption of Mn(II), Co(II), Ni(II), Zn(II), Cd(II), Eu(III), Am(III), Sn(IV), Th(IV), Np(V) and U(VI) on montmorillonite: Linear free energy relationships and estimates of surface binding constants for some selected heavy metals and actinides. *Geochim. Cosmochim. Acta* **2005**, 69 (4), 875–892.

(3) Pabalan, R.; Turner, D. R. Uranium (6+) sorption on montmorillonite: experimental and surface complexation modeling study. *Aquatic Geochem*. **1998**, 2(3), 203-226.

(4) Turner, D. R.; Sassman, S. A. Approaches to sorption modeling for high-level waste performance assessment. *J. Contam. Hydrol.* **1996**, 21, 311–332.

(5) McKinley, J. P.; Zachara, J. M.; Smith, S. C.; Turner, G. D. The influence of uranyl hydrolysis and multiple site-binding reactions on adsorption of U(VI) to montmorillonite. *Clays Clay Miner.* **1995**, 43, 586-598.

(6) Chisholm-Brause, C.; Conradson, S. D.; Buscher, C. T.; Eller, P. G.; Morris, D. E. Speciation of uranyl sorbed at multiple binding sites on montmorillonite. *Geochim. Cosmochim. Acta* **1994**, 58, 3625–3631.

(7) Schlegel, M.; Descostes, M. Uranium uptake by hectorite and montmorillonite: a solution chemistry and polarized EXAFS study. *Environ. Sci. Technol.* **2009**, 43 (22), 8593-8598.

(8) Catalano, J. G.; Brown B. G. Jr. Uranyl adsorption onto montmorillonite: Evaluation of binding sites and carbonate complexation. *Geochim. Cosmochim. Acta* **2005**, 69 (12), 2995-3005.

(9) Greathouse, J. A.; Cygan, R. T. Molecular dynamics simulation of uranyl(VI) adsorption equilibria onto an external montmorillonite surface. Phys. Chem. Chem. Phys. **2005**, 7 (20), 3580-3586.

(10) Kowal-Fouchard, A.; Drot, R.; Simoni, E.; Ehrhardt, J. J. Use of spectroscopic techniques for uranium(VI)/montmorillonite interaction modelling. *Environ. Sci. Technol.* **2004**, 38 (5), 1399-1407.

(11) Zaidan, O. F.; Greathouse, J. A.; Pabalan, R. T. Monte Carlo and molecular dynamics simulation of uranyl adsorption on montmorillonite clay. *Clays Clay Miner.* **2003**, 51, 372–381.

(12) Hennig, C.; Reich, T.; Dähn, R.; Scheidegger, A. M. Structure of uranium sorption complexes at montmorillonite edge sites. *Radiochim. Acta* **2002**, 90 (9), 653-657.

(13) Sylwester, E. R.; Hudson, E. A.; Allen, P. G. The structure of uranium (VI) sorption complexes on silica, alumina, and montmorillonite. *Geochim. Cosmochim. Acta* **2000**, 64 (14), 2431-2438.

(14) Dent, A. J.; Ramsay, J. D. F.; Swanton, S. W.; An EXAFS study of uranyl ion in solution and sorbed onto silica and montmorillonite clay colloids. *J. Colloid Interface Sci.* **1992**, 150 (1), 45-60.

(15) Tsarev, S.; Waite, T. D.; Collins, N. R. Uranium reduction by Fe(II) in the presence of montmorillonite and nontronite. *Environ. Sci. Technol.* **2016**, 50, 15, 8223-8230.

(16) Zhang, G.; Senko, J. M.; Kelly, S. D.; Tan, H.; Kemner, K. M.; Burgos, W. B. Microbial reduction of iron(III)-rich nontronite and uranium(VI). *Geochim. Cosmochim. Acta* **2009**, 73 (12), 3523-3538.

(17) Ames, L. L.; McGarrah, J. E.; Walker, B. A.; Salter, P. F. Sorption of trace constituents from aqueous solutions onto secondary minerals. I. uranium. *Clays Clay Miner.* **1983**, 31 (5), 321-334.

(18) Hofstetter, T. B.; Neumann, A.; Schwarzenbach, R. P. Reduction of nitroaromatic compounds by Fe(II) species associated with iron-rich smectites. *Environ. Sci. Technol.* **2006**, 40, 235-242.

(19) Charlet, L.; Scheinost, A. C.; Tournassat, C.; Greneche, J. M.; Géhin, A.; Fernández-Martínez, A.; Coudert, S.; Tisserand, D.; Brendle, J. Electron transfer at the mineral/water interface: selenium reduction by ferrous iron sorbed on clay. *Geochim.Cosmochim. Acta* **2007**, *71*, 5731-5749.

(20) Neumann, A.; Hofstetter, T. B.; Skarpeli-Liati, M.; Schwarzenbach, R. P. Reduction of polychlorinated ethanes and carbon tetrachloride by structural Fe(II) in smectites. *Environ. Sci. Technol.* **2009**, 43, 4082-4089.

(21) Géhin, A.; Grenèche, J. M.; Tournassat, C.; Brendlé, J.; Rancourt, D. G.; Charlet, L. Reversible surface-sorption-induced electron-transfer oxidation of Fe(II) at reactive sites on a synthetic clay mineral. *Geochim. Cosmochim. Acta* **2007**, 71, 863–876.

(22) Schultz, C. A.; Grundl, T. J. pH dependence of ferrous sorption on two smectite clays. *Chemosphere*, **2004**, 57, 1301-1306.

(23) Soltermann, D.; Fernandes, M. M.; Baeyens, B.; Dähn, R.; Joshi, P. A.; Scheinost, A. C.; Gorski, C. A. Fe(II) uptake on natural montmorillonites. I. macroscopic and spectroscopic characterization. Environ. Sci. Technol. **2014**, 48 (15), 8688-8697.

(24) Jaisi, D.P.; Dong, H.; Morton, J. P. Partitioning of Fe(II) in reduced nontronite (NAu-2) to reactive sites: reactivity in terms of Tc(VII) reduction. *Clays Clay Miner.* **2008**, 56 (2), 175-189.

(25) Chakraborty, S.; Favre, F.; Banerjee, D.; Scheinost, A. C.; Mullet, M.; Ehrhardt, J. J.; Brendle, J.; Vidal, L.; Charlet, L. U(VI) sorption and reduction by Fe(II) sorbed on montmorillonite. *Environ. Sci. Technol.* **2010**, 44 (10), 3779-3785.

(26) Schultz, C. A.; Grundl, T. J. pH dependence on reduction rate of 4-Cl-nitrobenzene by Fe(II)/ montmorillonite systems. *Environ. Sci. Technol.* **2000**, 34, 3641-3648.

(27) Jones, A. M.; Murphy, C. A.; Waite T. D.; Collins, A. N. Fe(II) interactions with smectites: temporal changes in redox reactivity and the formation of green rust. *Environ. Sci. Technol.* **2017** 51 (21), 12573-12582.

(28) Merola, R. B.; Fournier, E. D.; McGuire, M. M. Spectroscopic investigations of Fe^{2+} complexation on nontronite clay. *Langmuir* **2007**, 23 (3), 1223-1226.

(29) Schaefer, M. V.; Gorski, C. A.; Scherer, M. M. Spectroscopic evidence for interfacial Fe(II)-Fe(III) electron transfer in a clay mineral. *Environ. Sci. Technol.* **2011**, 45, 540–545.

(30) Neumann, A.; Olson, T. L.; Scherer, M. M. Spectroscopic evidence for Fe(II)−Fe(III) electron transfer at clay mineral edge and basal sites. *Environ. Sci. Technol.* **2013**, 47 (13), 6969-6977.

(31) Latta, D. E.; Neumann, A.; Premaratne, W. A. J.; Scherer, M. Fe(II)-Fe(III) electron transfer in a clay mineral with low Fe content. *ACS Earth Space Chem.* **2017**, 1 (4), 197-208.

(32) Ilgen, A. G.; Kruichak, J. N.; Artyushkova, K.; Newville, M. G.; Sun, C. Redox transformations of As and Se at the surfaces of natural and synthetic ferric nontronites: role of structural and adsorbed Fe(II). *Environ Sci Technol.* **2017**, 51 (19), 11105-11114.

(33) Morgan, B.; Lahav, O. The effect of pH on the kinetics of spontaneous Fe(II) oxidation by O_2 in aqueous solution-basic principles and a simple heuristic description. *Chemosphere* **2007**, 68, 2080-2084.

(34) Gates, W. P.; Slade, P. G.; Manceau, A.; Lanson, B. Site occupancies by iron in nontronites. *Clays Clay Miner.* **2002**, 50 (2), 223-239.

(35) Varret, F. ; Teillet, J. Unpublished Mosfit program, Université du Maine, France.

(36) Webb, S. M. SIXPack: a graphical user interface for XAS analysis using IFEFFIT. *Physica Scripta* **2005**, T115, 1011-1014.

(37) Ressler, T. WinXAS: a program for X-ray absorption spectroscopy data analysis under MS Windows. *J. Synchr. Radiat.* **1998**, 5, 118-122.

(38) Rossberg, A.; Reich, T.; Bernhard, G., Complexation of uranium(VI) with protocatechuic acid - application of iterative transformation factor analysis to EXAFS spectroscopy. *Anal. Bioanal. Chem.* **2003**, 376 (5), 631-638.

(39) Rossberg, A.; Ulrich, K.-U.; Weiss, S.; Tsushima, S.; Hiemstra, T.; Scheinost, A. C., Identification of uranyl surface complexes on ferrihydrite: Advanced EXAFS data analysis and CD-MUSIC modeling. *Environ. Sci. Technol.* **2009**, 43 (5), 1400–1406.

(40) Lucks, C.; Rossberg, A.; Tsushima, S.; Foerstendorf, H.; Scheinost, A. C.; Bernhard, G., Aqueous Uranium(VI) Complexes with Acetic and Succinic Acid: Speciation and Structure Revisited. *Inorg. Chem.* **2012**, 51 (22), 12288-12300.

(41) Allen, P. G.; Shuh, D. K.; Bucher, J. J.; Edelstein, N. M.; Palmer, C. E. A.; Silva, R. J.; Nguyen, S. N.; Marquez, L. N.; Hudson, E. A. Determination of uranium structures by EXAFS: schoepite and other U(VI) oxide precipitates. *Radiochim. Acta* **1996**, 75, 47–53.

(42) Truche, L.; Joubert, G.; Dargent, M.; Martz, P., Cathelineau, M., Rigaudier, T., Quirt, D. Clay minerals trap hydrogen in the Earth's crust: Evidence from the Cigar Lake uranium deposit, Athabasca. *Earth Planetary Sci. Lett.* **2018**, 493, 186–197.

(43) Chakraborty, S.; Bardelli, F.; Mullet, M.; Greneche, J. M.; Varma, S.; Ehrhardt, J. J.; Banerjee, D.; Charlet, L. Spectroscopic studies of arsenic retention onto biotite. *Chem. Geol.* **2011**, 281 (1-2), 83-92.

TABLE 1. Experimental conditions of sorption of U(VI) on Fe(II) sorbed onto smectite clays[a]

Sample No.	Clay type	$[Fe(II)]_0$ (mmolL^{-1})	pH_{i_Fe}	$[Fe(II)]_{sorb}$ (mmolkg^{-1})	$[U(VI)]_0$ (mmolL^{-1})	pH_{i_U}	pH_{f_U}	$[U(VI)]_{sorb}$ (mmolkg^{-1})
M[c]	Fe-free (0 wt%) montmorillonite (MONT)	1.24	6.0	20.5	-	-	-	-
M1		-	-	-	0.13	6.0	6.3	12.1
M2[c]		1.15	5.9	19.7	0.13	6.0	6.1	12.0
M3		1.21	6.0	20.6	0.13	6.0	6.0	11.8
U1[b]		0.69	6.2	20.0	0.04	6.1	5.5	8.3
F	Fe-poor (2.6 wt%) montmorillonite (Fe-MONT)	1.50	5.9	87.3	-	-	-	-
F1		-	-	-	0.11	5.8	5.7	9.5
F2		1.50	5.9	85.7	0.13	6.0	5.7	8.8
N	Fe-rich (25.8 wt%) nontronite (NAu-2)	1.08	6.0	103.3	-	-	-	-
N1		-	-	-	0.13	6.2	5.1	11.8
N2		1.11	6.0	103.5	0.14	5.9	5.3	10.4

[a] [clay] =10.6 ± 0.2 gL^{-1}, M & U = montmorillonite (MONT); F = Fe-montmorillonite (Fe-MONT) and N = Nontronite (NAu-2); equilibration time of Fe(II) with clay before U(VI) addition = 72 h and equilibration time of U(VI) after Fe(II) sorption on clay = 72 h.

[b] study by Chakraborty et al.[25]

[c] samples prepared using $^{57}Fe(II)$

TABLE 2. Quantification of U(VI) precipitation molar fraction as soddyite-like mineral phase and U(VI) sorbed as obtained by ITFA of XANES (12.10–12.25 keV).

Sample No	**pH**	**t (hr)**	**U(VI) precipitated as soddyite-like phase $(UO_2)_2SiO_4.2H_2O$**	**U(VI) sorbed onto Fe(II) sorbed on clays**	**Sum**
Soddyite	-	-	1.00	0.00	1.00
M1	6.0	72	0.00	1.00	1.00
M2a	5.8	0.16	0.02	0.97	0.99
M2b	5.7	1	0.05	0.92	0.98
M2c	5.5	24	0.08	0.87	0.95
M2	6.0	72	0.26	0.51	0.77
M3	6.0	72	0.75	0.00	0.75
F1	5.8	72	0.08	0.89	0.97
F2	6.0	72	0.03	0.92	0.95
N1	-	-	0.00	1.00	1.00
N2	5.9	72	0.04	0.99	1.03

TABLE 3. Quantification of U oxidation states (molar fraction) by ITFA of XANES (12.10–12.25 keV) and solution data (pH, [Si], [U] in µmolL^{-1}).

Sample No	pH	t (hr)	U(VI)	U(IV)	Sum	$[Si]_{solution}$ in µmolL^{-1}	$[U]_{solution}$ in µmolL^{-1}
M1	6.0	72	1.00	0.00	1.00	-	-
M2a	5.8	0.16	0.94	0.06	0.99	345	11
M2b	5.7	1	0.95	0.05	1.00	351	20
M2c	5.5	24	0.79	0.21	1.00	358	18
M2	6.0	72	0.91	0.09	1.00	335	3
U1[a]	6.1	72	0.87	0.14	1.01	-	-

[a] Study by Chakraborty et al.[25]

TABLE 4. Refined values of [57]Mössbauer hyperfine parameters estimated from the spectra presented in Figure 4.

Sample No.	Site		$\delta \pm$ 0.02	$\Gamma \pm$ 0.02	$\Delta E_Q \pm$ 0.02	RA ± 2
M (Fe(II)/MONT)	Fe(II)_exch_$FeCl^+$	D1	1.37	0.41	3.40	36
	Fe(II)_exch_Fe^{2+}	D2	1.32	0.34	3.03	33
	Fe(II)_strong_red2	D3	1.28	0.34	2.62	21
	Fe(III)_strong_ox	D4	0.47	0.49	0.58	10
M2c (Fe(II)/MONT+U(VI))	Fe(II)_exch_$FeCl^+$	D1	1.37	0.28	3.42	39
	Fe(II)_exch_Fe^{2+}	D2	1.34	0.38	3.04	32
	Fe(II)_strong_red2	D3	1.30	0.32	2.59	13
	Fe(III)_strong_ox	D4	0.47	0.46	0.58	10
	Fe(III)_strong_red2	D5	0.48	0.46	1.24	6

δ (mm s^{-1}) isomer shift with respect to metallic α-Fe(0) at 300K; ΔE_Q (mm s^{-1}) quadrupole splitting; RA (%) relative abundance, Γ (mm s^{-1}) full-width at half-height.

FIGURE CAPTIONS

Figure 1. Kinetics of U(VI) sorption on (A) Fe(II)/MONT; (B) Fe(II)/Fe-MONT, Fe(II)/NAu-2. [U(VI) added to Fe(II)/clay suspensions at t = 0].

Figure 2. U L_{III}-edge XAS spectra of U(VI) sorbed on MONT, Fe-MONT and NAu-2 in the presence of Fe(II) compared to the U(VI) and soddyite references, (A) fitted XANES; (B) EXAFS and (C) Fourier transform of EXAFS.

Figure 3. U L_{III}-edge XAS spectra of kinetics of U(VI) sorption on MONT in the presence of Fe(II) compared to the U(VI) (M1 sample in Table 1) and U(IV) colloid references, (A) fitted XANES; (B) EXAFS and (C) Fourier transform of EXAFS.

Figure 4. ^{77}K Mössbauer spectra of ^{57}Fe(II) sorbed on MONT (A) before; (B) after U(VI) addition.

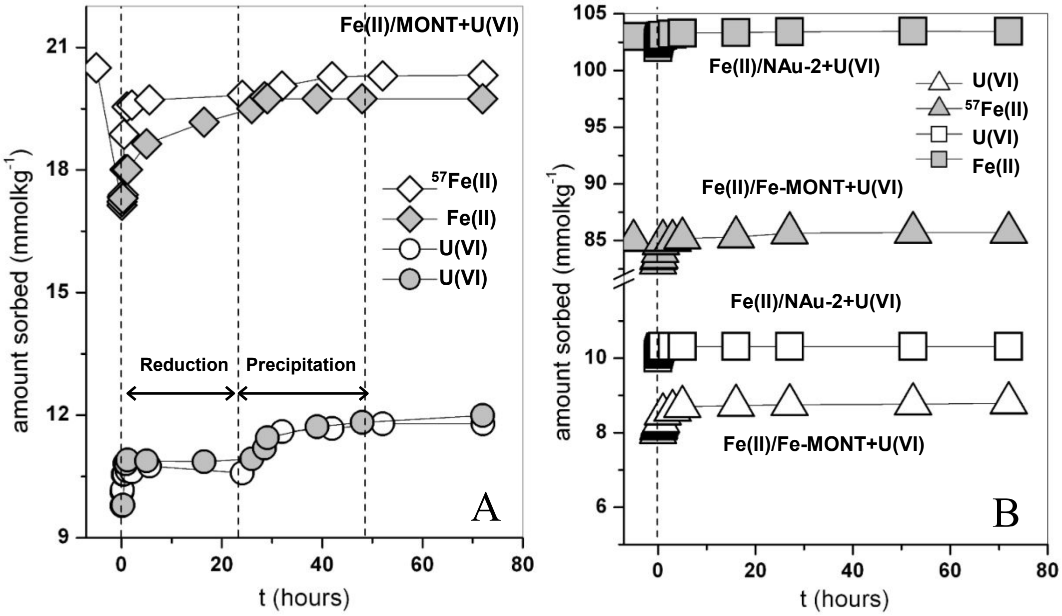
Fe(II)/MONT+U(VI)
^{57}Fe(II)
Fe(II)
U(VI)
U(VI)
Reduction
Precipitation
amount sorbed (mmolkg^{-1})
t (hours)
A
Fe(II)/NAu-2+U(VI)
U(VI)
^{57}Fe(II)
U(VI)
Fe(II)
Fe(II)/Fe-MONT+U(VI)
Fe(II)/NAu-2+U(VI)
Fe(II)/Fe-MONT+U(VI)
amount sorbed (mmolkg^{-1})
t (hours)
B

Figure 1

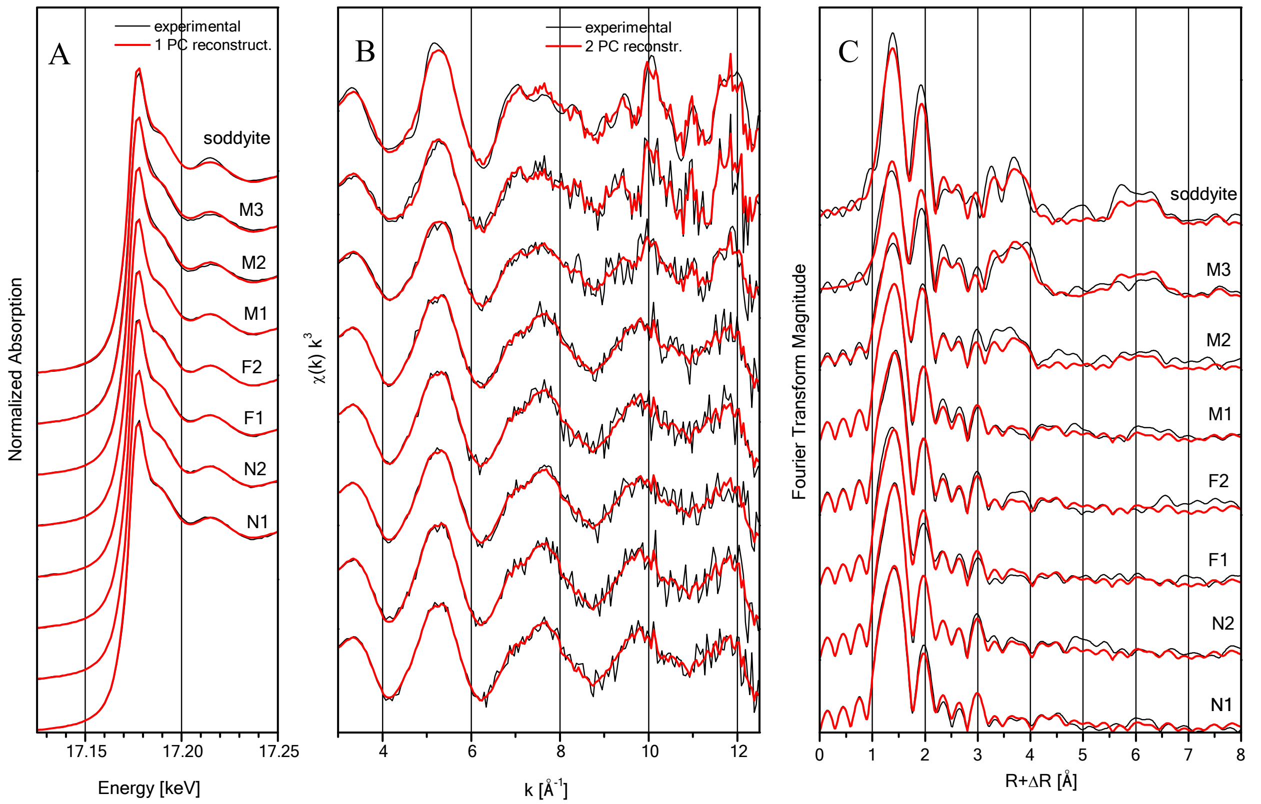
A
experimental
1 PC reconstruct.
soddyite
M3
M2
M1
F2
F1
N2
N1
Normalized Absorption
17.15
17.20
17.25
Energy [keV]
B
experimental
2 PC reconstr.
χ(k) k³
4
6
8
10
12
k [Å⁻¹]
C
soddyite
M3
M2
M1
F2
F1
N2
N1
Fourier Transform Magnitude
0
1
2
3
4
5
6
7
8
R+ΔR [Å]

Figure 2

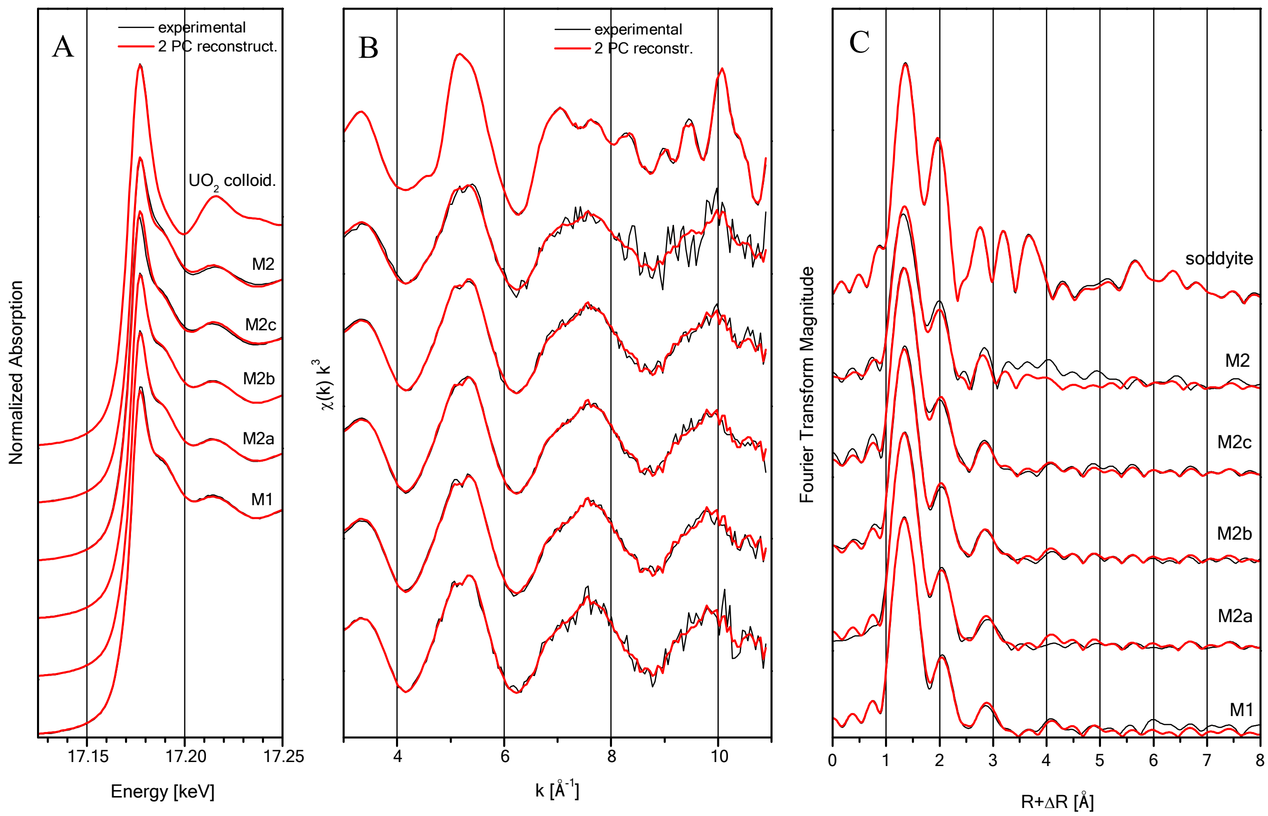
A
experimental
2 PC reconstruct.
UO2 colloid.
M2
M2c
M2b
M2a
M1
Normalized Absorption
17.15
17.20
17.25
Energy [keV]
B
experimental
2 PC reconstr.
χ(k) k3
4
6
8
10
k [Å-1]
C
soddyite
M2
M2c
M2b
M2a
M1
Fourier Transform Magnitude
0
1
2
3
4
5
6
7
8
R+ΔR [Å]

Figure 3

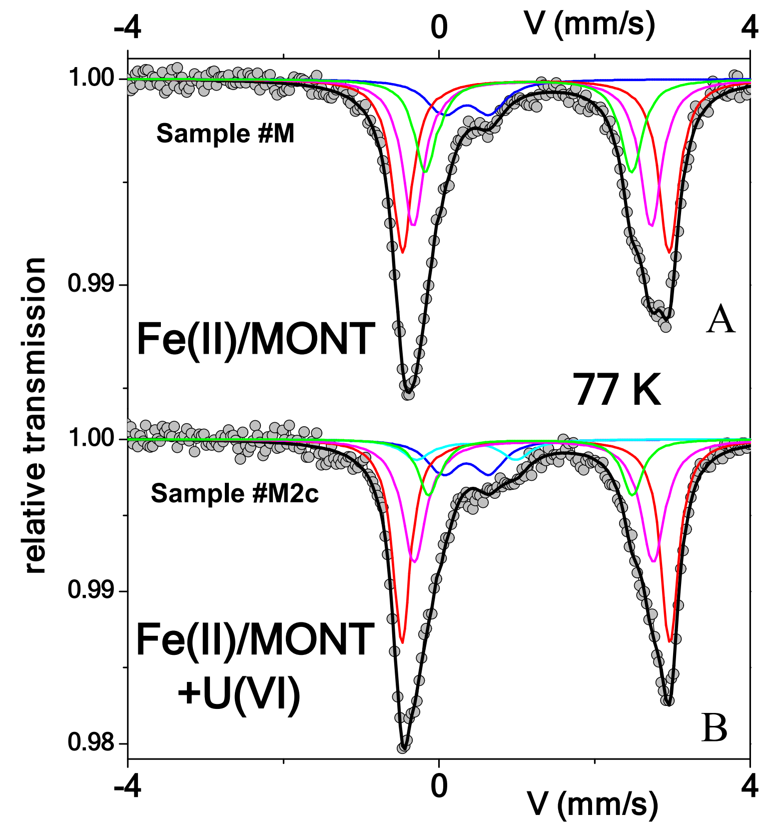
-4
0
V (mm/s)
4
1.00
Sample #M
0.99
Fe(II)/MONT
A
77 K
1.00
Sample #M2c
0.99
Fe(II)/MONT
+U(VI)
0.98
B
-4
0
V (mm/s)
4
relative transmission

Figure 4